Disrupted coupling of gating charge displacement to Na^+ current activation for DIIS4 mutations in hypokalemic periodic paralysis

Wentao Mi, Volodymyr Rybalchenko, and Stephen C. Cannon

Department of Neurology and Neurotherapeutics, University of Texas Southwestern Medical Center, Dallas, TX 75390

Missense mutations at arginine residues in the S4 voltage-sensor domains of $Na_V1.4$ are an established cause of hypokalemic periodic paralysis, an inherited disorder of skeletal muscle involving recurrent episodes of weakness in conjunction with low serum K^+. Expression studies in oocytes have revealed anomalous, hyperpolarization-activated gating pore currents in mutant channels. This aberrant gating pore conductance creates a small inward current at the resting potential that is thought to contribute to susceptibility to depolarization in low K^+ during attacks of weakness. A critical component of this hypothesis is the magnitude of the gating pore conductance relative to other conductances that are active at the resting potential in mammalian muscle: large enough to favor episodes of paradoxical depolarization in low K^+, yet not so large as to permanently depolarize the fiber. To improve the estimate of the specific conductance for the gating pore in affected muscle, we sequentially measured Na^+ current through the channel pore, gating pore current, and gating charge displacement in oocytes expressing R669H, R672G, or wild-type $Na_V1.4$ channels. The relative conductance of the gating pore to that of the pore domain pathway for Na^+ was 0.03%, which implies a specific conductance in muscle from heterozygous patients of ~10 $\mu S/cm^2$ or 1% of the total resting conductance.

Unexpectedly, our data also revealed a substantial decoupling between gating charge displacement and peak Na^+ current for both R669H and R672G mutant channels. This decoupling predicts a reduced Na^+ current density in affected muscle, consistent with the observations that the maximal dV/dt and peak amplitude of the action potential are reduced in fibers from patients with R672G and in a knock-in mouse model of R669H. The defective coupling between gating charge displacement and channel activation identifies a previously unappreciated mechanism that contributes to the reduced excitability of affected fibers seen with these mutations and possibly with other R/X mutations of S4 of Na_V, Ca_V, and K_V channels associated with human disease.

INTRODUCTION

Hypokalemic periodic paralysis (HypoPP) is a dominantly inherited disorder of skeletal muscle with recurrent episodes of weakness in association with low serum K^+ (Lehmann-Horn et al., 2004; Cannon, 2006). Missense mutations of $Na_V1.4$ and $Ca_V1.1$ are established causes of HypoPP. A final common pathway for the mechanistic basis of weakness is paradoxical depolarization of muscle fibers in low K^+ (often <3 mM), which inactivates $Na_V1.4$ and renders fibers refractory and inexcitable (Rüdel et al., 1984). Remarkably, all 10 HypoPP mutations reported in $Na_V1.4$ are missense substitutions at arginine residues in the outer end of S4 segments in domains I–III of the voltage sensors (Matthews et al., 2009). Six of the $Ca_V1.1$ HypoPP mutations are also at arginine residues in S4 segments. Expression studies in oocytes (Sokolov et al., 2007; Struyk and Cannon, 2007; Struyk et al., 2008; Francis et al., 2011) and knock-in mutant mouse models (Wu et al., 2011, 2012) have implicated a common functional defect, wherein the R/X missense mutations in S4 segments produce an aberrant ion conduction pathway in the voltage-sensor domain that allows an influx of current at the resting potential. This so-called omega current or gating pore current, I_{GP}, is very small compared with the ionic current conducted by the pore domain. Computer simulations have demonstrated that even small gating pore currents may increase the susceptibility to paradoxical depolarization at low K^+, where the outward current contribution for the inward rectifier ($V_{rest} > E_K$) becomes overwhelmed by the inward gating pore leakage current (Struyk and Cannon, 2008; Jurkat-Rott et al., 2010).

A critical question in establishing the gating pore current as a major contributor to the pathogenesis of transient weakness in HypoPP has been, what is the relative conductance or current density of I_{GP} compared with the normal ionic conductances that regulate excitability of skeletal muscle? Extrapolation of oocyte expression data, based on a few fortuitous measurements of both ionic Na^+ current, I_{Na}, and I_{GP} in an oocyte expressing $Na_V1.4$-R672G, led to the conclusion that I_{GP} at the

Correspondence to Stephen C. Cannon: steve.cannon@utsouthwestern.edu

Abbreviations used in this paper: HypoPP, hypokalemic periodic paralysis; TTX, tetrodotoxin.

The Rockefeller University Press $30.00
J. Gen. Physiol. Vol. 144 No. 2 137–145
www.jgp.org/cgi/doi/10.1085/jgp.201411199

resting potential (−90 mV) was ∼1.25% of the I_{Na} peak during an action potential (Sokolov et al., 2007). Our estimate, based on a comparison of maximal gating charge displacement to I_{GP} for oocytes expressing $Na_V1.4$-R669H, was ∼10-fold smaller (Struyk and Cannon, 2007). Was this difference intrinsic to the particular mutation? The R672G mutation creates a nonselective cation conductance permeable to Na^+, K^+, and even $NMDG^+$, whereas R669H produces a proton-selective conduction pathway. Or, is the discrepancy the result of different methods used to extrapolate the oocyte data to the situation in mammalian skeletal muscle? We sought to resolve this discrepancy and to gain an improved estimate for the predicted gating pore conductance in HypoPP muscle fibers by measuring the Na^+ current, maximal on-gating charge displacement, and gating pore current all from the same oocyte expressing R669H, R672G, or WT $Na_V1.4$ channels. An analysis of these measurements provided a consensus for quantifying the relative magnitude of I_{GP}. The predicted specific conductance of the gating pore in HypoPP muscle was comparable to experimental values obtained in voltage-clamp studies of our knock-in mouse model of $Na_V1.4$-R669H HypoPP. Unexpectedly, we also observed a substantial decoupling between gating charge displacement and peak ionic current for both HypoPP mutant channels. This decoupling identifies a new mechanism by which excitability may be reduced in HypoPP fibers and accounts for the experimental observation that peak dV/dt and action potential overshoot in muscle are reduced in human HypoPP fibers (Jurkat-Rott et al., 2000) and in the $Na_V1.4$-R669H knock-in mouse (Wu et al., 2011).

MATERIALS AND METHODS

Expression of $Na_V1.4$ channels in oocytes

The rat adult skeletal muscle Na^+ channel α subunit, $rNa_V1.4$, was coexpressed with the human β1 subunit in *Xenopus laevis* oocytes. WT and mutant α-subunit constructs were created in the vector pGEMHE, as described previously (Struyk and Cannon, 2007; Struyk et al., 2008), to promote high expression levels in oocytes. To facilitate comparisons with other studies on HypoPP in humans, we named the mutant constructs in this paper for their disease-associated orthologues in human $Na_V1.4$. The $rNa_V1.4$-R663H mutation in the outermost arginine of S4 in domain II is denoted as R669H, and $rNa_V1.4$-R666G is denoted as R672G. cRNAs were synthesized by in vitro transcription using the mMessage mMachine kit (Ambion), and oocytes were injected with ∼50 ng of cRNA encoding either WT or mutant $Na_V1.4$, together with ∼50 ng of β1-subunit transcript (approximately fourfold molar excess). Oocytes were either obtained commercially (EcoCyte) or harvested by partial oophorectomy. Frogs, *Xenopus*, were housed in an Association for Assessment and Accreditation of Laboratory Animal Care–accredited facility, and all experiments were performed within guidelines established by the University of Texas Southwestern Medical Center Institutional Animal Care and Use Committee. Injected oocytes were maintained at 18°C in 0.5× Leibovitz's L-15 medium (HyClone) supplemented with 1% horse serum, 100 U/ml penicillin, 100 µg/ml streptomycin, and 100 µg/ml amikacin.

Electrophysiology

In all experiments, oocytes were voltage clamped in the cut-open configuration, with active clamping of the upper and guard chambers using an amplifier (CA-1B; Dagan Corporation) in headstage clamp mode. A perfusion manifold was built to allow complete exchange of the bath in the upper and lower chambers. Low resistance access to the intracellular compartment was obtained by permeabilizing the oocyte membrane in the lower chamber with 0.04% saponin. An equilibration period of >30 min was used to dialyze the oocyte intracellular contents with the lower chamber solution before recording currents. Computer control of command potentials and data acquisition were performed with an interface (ITC-1600; HEKA) using custom software developed in our laboratory.

The voltage-sensing electrode was fabricated from thin-walled borosilicate glass, filled with 3 M KCl, and positioned just under the dome of oocyte membrane in the upper chamber. Electrical connections to the three chambers were made with agarose-filled capillary bridges containing 110 mM Na^+ methanesulfonate and 10 mM HEPES, pH 7.4, and threaded with platinum wire. For experiments to measure gating charge displacement currents, compensation for linear capacitance transients was made with the amplifier's analogue circuitry. No analogue compensation for linear leakage current was used. Current signals were low-pass filtered at 5 kHz and sampled at 50 kHz.

All recordings were performed in Cl^--free solutions to minimize the contribution from anion conductances endogenous to the oocyte. The oocyte internal solution was equilibrated with the lower guard chamber containing (mM): 120 KOH, 10 EGTA, and 10 HEPES, pH 7.4 with methane sulfonate. In some experiments, KOH was replaced by NMDG. The upper chamber solution was initially high Na^+ to record ionic Na^+ currents conducted through the conventional pore (mM): 115 NaOH, 3 KOH, 1.5 $Ca(OH)_2$, 2.5 $Ba(OH)_2$, and 10 HEPES, pH 7.4 with methane sulfonate. Gating pore (omega) currents were then recorded from the same oocyte by replacing the external solution for which Na^+ was substituted with an equimolar amount of K^+ plus 1 µM tetrodotoxin (TTX). For some experiments, to isolate the gating change displacement current, an NMDG-based external bath was used (1 µM TTX plus [mM]: 113 NMDG, 1.5 $Ca(OH)_2$, 2.5 $Ba(OH)_2$, and 10 HEPES, pH 7.4 with methane sulfonate).

Data analysis

Peak and steady-state current levels were extracted from current tracings using custom software. Gating pore ionic currents were isolated in oocytes expressing mutant channels by subtracting the average current–voltage response for oocytes expressing WT channels in the presence of TTX, as described previously (Struyk and Cannon, 2007). Gating currents were quantified as the nonlinear charge displacement, Q_{on}, in response to step depolarization from a holding potential of −100 mV. Q_{on} was calculated by integration of the leak-subtracted current transient elicited by a 50-msec step depolarization. The leakage current was measured for a small 10-mV depolarization from a holding potential of −100 mV, for which the gating charge contribution was miniscule. This leakage current was digitally scaled and subtracted from raw current records to obtain P/N leak-subtracted traces. Additional compensation for nonlinear contributions from incomplete block of ionic Na^+ currents or in conditions with substantial gating pore currents was performed by offline subtraction (see Online supplemental material below). The Q_{on}–V relation for a series of test voltages was then fit with a Boltzmann distribution to determine the maximal gating charge displacement, Q_{on_max}, as channels transitioned from fully closed to fully open:

$$Q_{on} = Q_{on\_max} \Big/ \left(1 + e^{-(V - V_{1/2})/k}\right),$$

where $V_{1/2}$ is the voltage of half-maximal charge movement, and k is a steepness factor. In all figures, error bars represent ± SEM.

Online supplemental material

The supplemental text describes baseline correction (see also Fig. S1) for persistent gating pore currents that may have caused a modest overestimate of on-gating charge displacement from the integrated current, especially for R672G mutant channels, but the error is <15%. The online supplemental material is available at http://www.jgp.org/cgi/content/full/jgp.201411199/DC1.

RESULTS

A primary objective of these experiments was to measure the conventional ionic Na^+ current (I_{Na}), the nonlinear gating charge displacement current (I_g), and for mutant channels, the ionic gating pore current (I_{GP}), all in the same oocyte. The motivation for these experiments was to gain a quantitative method to translate the magnitude of the anomalous gating pore currents observed for mutant $Na_V1.4$ channels expressed in oocytes to a predicted current density or specific conductance for the gating pore current in human HypoPP muscle fibers. Optimization of the experimental conditions was challenging because the high expression level required for detecting both the nonlinear charge displacement currents as well as gating pore currents resulted in space-clamp and series-resistance distortion of the ionic Na^+ currents, which were enormous. Low Na^+ solutions were not used to reduce voltage-clamp errors because permeant ion concentration has a marked effect on peak open probability (Townsend et al., 1997) and slow inactivation gating of $Na_V1.4$ (Townsend and Horn, 1997), and we did not want to assume that the peak I_{Na} would scale linearly with Na^+ concentration. Nor did we want to use partial block with

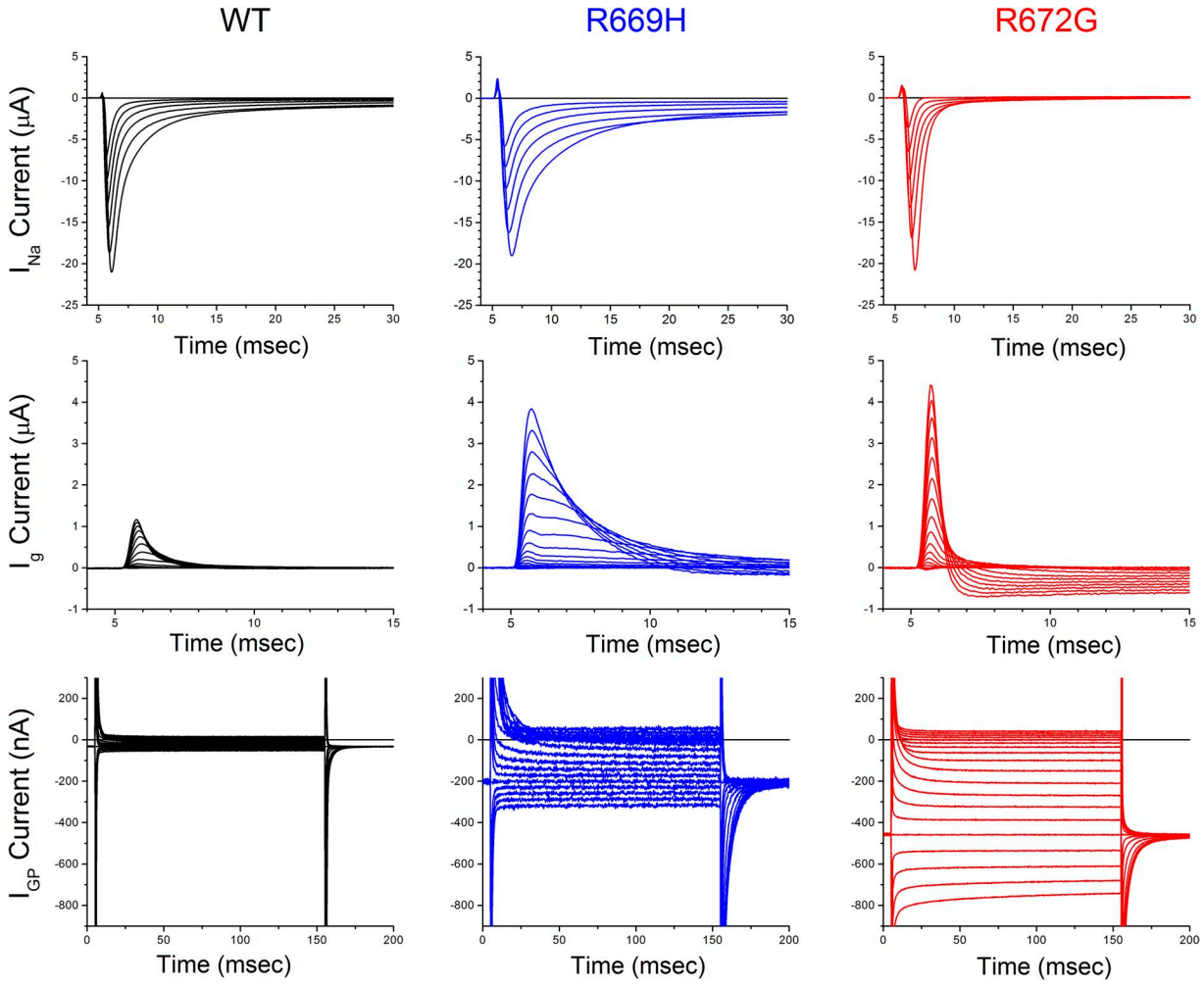

Figure 1. Currents, recorded under different conditions for the same oocyte, to measure I_{Na}, I_g, and I_{GP}. First, Na^+ currents were recorded in a 115-mM Na^+ bath with analogue compensation for linear capacitance and digital P/N subtraction of residual linear leak (top row). Responses are shown for test potentials of −20 to 30 mV. The external solution was then exchanged with K^+/TTX (R672G) or $NMDG^+$/TTX (R669H or WT), and P/N leak subtraction was performed to reveal the nonlinear gating charge displacement current, I_g (middle row). Finally, all analogue and digital P/N leak subtraction was omitted to reveal the gating pore current for mutant channels and the residual leakage current for oocytes expressing WT channels (bottom row). Each column shows the responses recorded from a single oocyte (black, WT; blue, R669H; red, R672G).

TTX, which would introduce another scale factor for relating I_{GP} to measured I_{Na}.

Fig. 1 shows a montage of representative I_{Na}, I_g, and I_{GP} currents, all recorded from one oocyte expressing WT, R669H, or R672G $Na_V1.4$ channels. Oocytes with similar peak I_{Na} current amplitudes were selected as a common basis for visual comparison. Display scales are identical across different channel types to facilitate a direct comparison of current amplitudes. The I_{Na} and I_g traces are P/N leak subtracted, whereas no digital subtraction has been performed on the I_{GP} traces in the bottom row. The current traces in a 115-mM Na^+ bath without TTX (Fig. 1, top row) show that for oocytes with peak inward I_{Na} amplitudes of 10–20 µA, an early outward transient was pronounced for the mutant channels compared with WT. We interpret these transients to be nonlinear gating charge displacement currents that were unexpectedly larger in mutant channels compared with WT. Unlike our previous studies in HEK cells (Struyk et al., 2000), the decay of I_{Na} for R669H mutants expressed in oocytes was markedly slower than WT. This slower rate of macroscopic inactivation was accompanied by slower kinetics for the on-gating charge (Fig. 1, middle row).

The external solution was then exchanged with an $NMDG^+$/TTX solution for R669H or a K^+/TTX solution for R672G and WT to suppress I_{Na} and record I_g and I_{GP}. The nonlinear charge displacement currents revealed by P/N leak subtraction (Fig. 1 middle row) were indeed substantially larger for oocytes expressing R669H and R672G channels that had I_{Na} amplitudes comparable to WT (Fig. 1, top row). For the sample I_g traces shown in Fig. 1, the maximal on-gating charge was Q_{on} = 0.90 nC for WT, 7.9 nC for R669H, and 2.8 nC for R672G. Pilot experiments with $NMDG^+$ substituted for Na^+, but without TTX, revealed very large nonlinear current transients in response to depolarization, with a similar appearance to on-gating charge displacement currents. We attribute this large current transient to egress of $NMDG^+$ from within the transmembrane electric field of $Na_V1.4$, most likely the outer pore because it was abolished by the addition of 1 µM TTX (apparent Q_{on_max} decreased fivefold with TTX; not depicted). Capes et al. (2012) reported this same effect and also noted that the addition of TTX reduced the off-gating charge by 24%. The exceptionally large nonlinear current transients for R669H (Fig. 1, center of middle row) are not attributable to this phenomenon because comparably large Ig currents for R669H were recorded in control conditions with K^+/TTX external solution. The steady-state inward current for R672G traces (Fig. 1, middle row) was caused by the gating pore current, which is permeable to $NMDG^+$ and not blocked by TTX. The paradoxical appearance of larger inward steady-state current with more positive test-pulse depolarizations was caused by the leak-subtraction method. The gating pore was open during measurement of the "leak" response at −100 mV, and then closed with depolarization, thereby resulting in overcompensation for the P/N leak subtraction. The contribution from the gating pore current, I_{GP}, is shown more clearly by the steady-state values for traces in which no leak or offset subtraction has been performed (Fig. 1, bottom row). The traces for WT show a small nonspecific linear leak compared with the inward-rectifying I_{GP} currents observed in HypoPP mutant channels.

The coupling of gating charge displacement to channel opening was quantified by normalizing peak I_{Na} to Q_{on_max}, both measured from the same oocyte, and then computing the population behavior across many experiments in separate oocytes. Fig. 2 shows the mean and SEM for the ratio of I_{Na}/Q_{on_max} over a series of test potentials from −80 to 40 mV. This ratio was reduced twofold at all voltages for R672G and fourfold for R669H compared with WT. The data for WT channels showed evidence for poor voltage clamp with a left shift of the voltage at which the inward peak I_{Na} was maximal and there was a steepened increase in voltage dependence for opening. Partial compensation for these effects was obtained by rejecting oocytes in which the peak I_{Na} occurred at a test potential more negative than −30 mV. The reductions in normalized current amplitude for mutant channels from WT in Fig. 2 cannot be accounted for by a bias from poorer quality voltage clamp of WT channels alone. First, the maximal raw current amplitudes spanned a comparable range ([in µA] WT: mean of −25.8, range of −5.6 to −49; R669H: mean of −14.7, range of −1.1 to −36; R672G: mean of −25.6, range of −5.4 to −42), and the main cause for the difference in the ratio was the large Q_{on_max} for mutants (mean values of, [in nC] WT: 1.4, range of 0.22 to 2.5; R669H: 4.4, range of 1.1 to 10.5; R672G: 3.6, range of 1.8 to 7.4). Second, a bias from

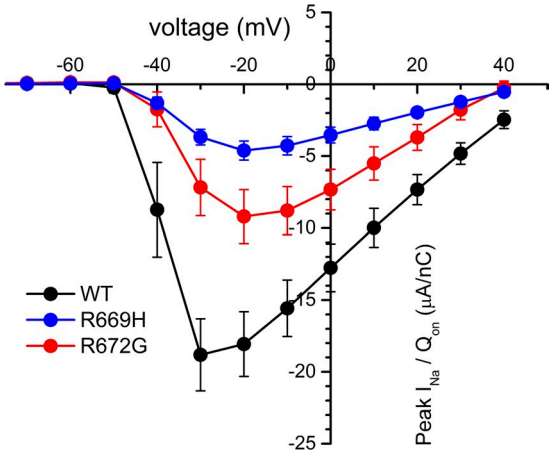

Figure 2. Voltage dependence for peak I_{Na}, normalized by maximal on-gating charge displacement, Q_{on_max}. Symbols show mean and SEM for WT (black; n = 15), R669H (blue; n = 34), and R672G (red; n = 18). Oocytes for which the maximal I_{Na} occurred at a voltage of less than −30 mV were excluded to reduce the effect of inadequate voltage-clamp control. Error bars represent ± SEM.

a greater loss of voltage-clamp control for WT channels would have caused a greater underestimate of I_{Na} amplitude compared with better clamped mutant channels, but just the opposite is shown in Fig. 2. Third, the reduced coupling ratio for mutant channels was prominent at strongly depolarized potentials (10–30 mV), where the voltage-clamp errors were much smaller because the peak amplitude of inward I_{Na} was much smaller.

The variability of the peak I_{Na} to Q_{on_max} relationship is shown in the scatter plot of Fig. 3 A, where each symbol is from a separate oocyte. The data for WT channels were tightly clustered to the expected linear relation (17.1 ± 1.1 μA/nC; $r^2 = 0.93$). For mutant channels, a linear relation was also found; however, the scatter was substantially greater (R669H: 2.81 ± 0.36 μA/nC, $r^2 = 0.63$; R672G: 6.46 ± 0.73 μA/nC, $r^2 = 0.77$). We interpret this variability for mutant channels as a stable disruption of charge displacement coupling to channel opening. Repeated measurements from the same oocyte showed a consistent coupling ratio over tens of minutes without evidence for rapid fluctuation. Perhaps this stable variability is caused by uncontrolled differences in separate oocytes, but there was no clustering of weak versus strong coupling within a single harvest of oocytes. Moreover, the coupling variability was absent from WT channels expressed in the same batch of oocytes. This suggests the possibility for a range of coupling states for HypoPP mutant channels, and that the rate of switching between these states is very slow. Another source of variability was rundown, with I_{Na} and Q_{on_max} both slowly decreasing over tens of minutes, but the ratio was stable. A statistical test for the difference in coupling efficiency of mutant channels from WT was made by ANOVA for the I_{Na}/Q_{on_max} ratio at the voltage where peak I_{Na} was maximal. The spread of these data are shown in the box plot of Fig. 3 B. The coupling of charge displacement to channel opening was reduced for both HypoPP mutant channels compared with WT ($P < 0.0001$), with R669H likely being more severe than R672G ($P = 0.027$).

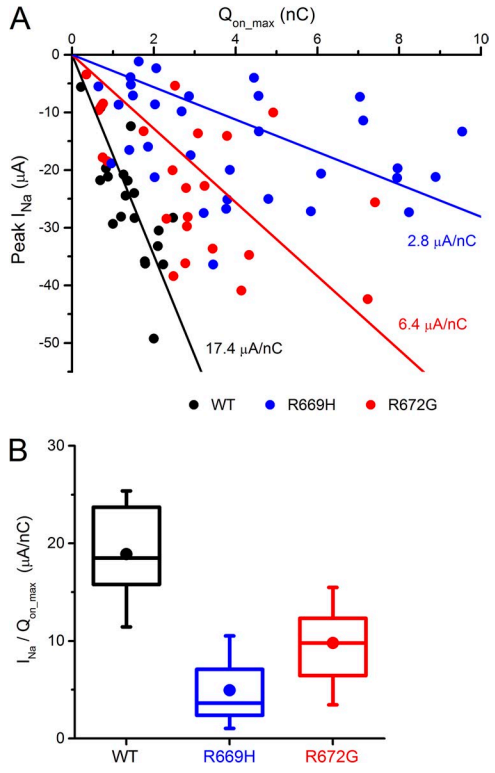

Figure 3. Coupling of gating charge displacement to peak ionic current is diminished and more variable for HypoPP mutants than for WT channels. (A) Each symbol represents the maximal peak I_{Na} and associated Q_{on_max} for a separate oocyte. Lines show the best fit constrained through the origin. (B) The ensemble coupling behavior for oocytes among each channel type is summarized in a box plot. For each oocyte, the ratio I_{Na}/Q_{on_max} was computed. Box plots show the mean (circle), 50% level (bar), 25–75% range (box), and 10–90% range (whiskers). The coupling ratio was lower for HypoPP mutant channels than in WT ($P < 0.0001$). Error bars represent ± SEM.

The steady-state amplitudes of the gating pore currents recorded from mutant channels are shown in Fig. 4. The current–voltage relation in Fig. 4 A shows an apparent inward rectification from the voltage dependence of the S4 displacement being in the permissive position for current flow, with an inward bias at negative membrane potentials. Currents are displayed as normalized I_{GP}/Q_{on_max} so that responses from separate oocytes with different expression levels can be combined. The normalized current density for the cation-nonselective R672G mutant was larger than for the proton-selective R669H mutant. The limiting slope conductance at the normal resting potential for muscle of −90 mV was 230 nS/nC for R669H and 560 nS/nC for R672G. The variability of I_{GP} amplitude with Q_{on_max} is shown in the scatter plot of Fig. 4 B. A linear relation was observed for both mutants (R669H: 25.6 ± 1.2 nA/nC, $r^2 = 0.93$; R672G: 99.1 ± 5.5 nA/nC, $r^2 = 0.95$). Importantly, these data are from the same oocytes for which the I_{Na}–Q_{on_max} relation is shown in Fig. 3. The coupling between gating charge movement and I_{GP} amplitude was highly correlated (Fig. 4), whereas the coupling between Q_{on_max} and channel opening for mutant channels showed substantial variability (Fig. 3). This observation suggests that every mutant channel at the surface membrane with a functioning voltage-sensor domain contributes to the gating pore leakage current, whereas not all mutant channels with functioning voltage sensors result in channel opening with depolarization.

DISCUSSION

Our efforts to measure I_{Na}, Q_{on_max}, and I_{GP} all from the same oocyte, for the purpose equating I_{GP} current density in the oocyte to a predicted density in human muscle fibers, led to the unexpected finding of a dissociation between I_{Na} amplitude and Q_{on_max} for both HypoPP mutant channels. The data convincingly show that the

ratio I_{Na}/Q_{on_max} is reduced for HypoPP mutants. The question is whether I_{Na} is smaller than expected or Q_{on_max} is too large. We favor the view that I_{Na} is smaller than normal. This hypothesis is consistent with the observation that dV/dt during the upstroke of the action potential is reduced in R672G human muscle (Jurkat-Rott et al., 2000). The basis for this apparent reduction in Na^+ current density was unknown, as the only recognized gating defect at that time was enhanced inactivation, and this should have been compensated by the protocol to hyperpolarize fibers before eliciting the action potential. The oocyte data in our study now show that for equivalent levels of expression in the membrane (as quantified by Q_{on_max}), the Na^+ current density would be reduced about twofold for R672G compared with WT. A similar finding was observed in our knock-in mutant mouse model of R669H (Wu et al., 2011). Heterozygous mutant mice had comparable transcript levels of WT and R669H alleles by RT-PCR, and yet dV/dt was reduced by 45% and the action potential amplitude was reduced by 29 mV. We interpret this relative reduction of I_{Na} compared with Q_{on_max} as a decoupling between voltage-sensor displacement to channel opening. The coupling defect appears to be noisy, with substantial variability from oocyte to oocyte (Fig. 3 A), but in the aggregate it is consistently reduced compared with WT channels. This defect had not been appreciated in prior expression studies of R669H or R672G in HEK cells (Jurkat-Rott et al., 2000; Struyk et al., 2000), because charge displacement currents were not measured in those studies. The observed mismatch of I_{Na} relative to Q_{on_max} for HypoPP mutant channels cannot be fully attributed to an overestimate of Q_{on_max} caused by the technical challenge of a superimposed I_{GP} current, because this error was at most 15% (supplemental text), whereas the ratio I_{Na}/Q_{on_max} was reduced 200% for R672H and 400% for R669H (Fig. 2). Our finding of a coupling defect could be a general mechanism by which mutations of arginine residues in S4 voltage sensors, as occurs in 14 of 15 published HypoPP mutations (Cannon, 2010), aggravate the susceptibility to failure of action potential propagation during an attack of periodic paralysis.

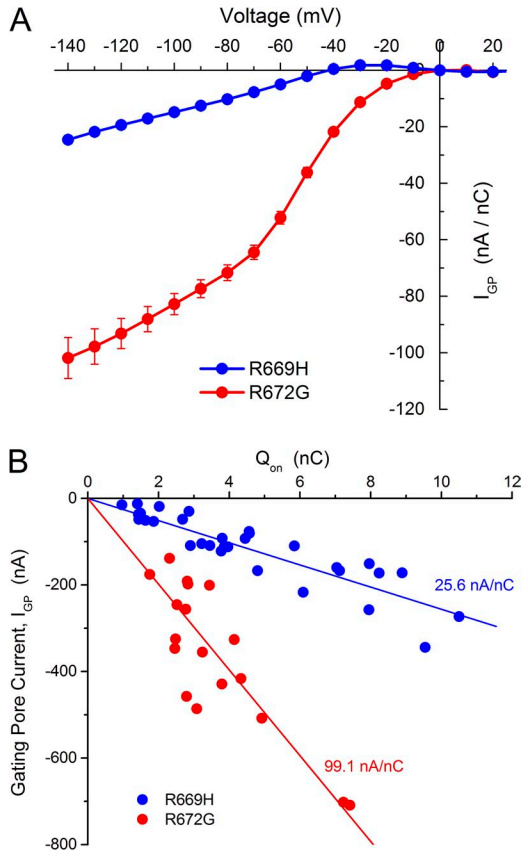

Figure 4. Gating pore currents in HypoPP mutant channels. (A) The gating pore current was measured as the steady-state current at the end of a 150-ms pulse that was leak corrected by subtraction of the average steady-state current recorded from oocytes expressing WT $Na_V1.4$. The gating pore current from each oocyte was normalized by Q_{on_max} for the same egg and plotted as a function of test potential. Symbols show mean and SEM for R669H mutants (blue; $n = 32$) and for R672G mutants (red; $n = 18$). Error bars represent ± SEM. (B) The correlation between the gating pore current measured at −140 mV and Q_{on_max} is shown as a scatter plot. Each symbol represents the response from a separate oocyte. Lines show the best fit constrained through the origin. The correlation for I_{GP}–Q_{on_max} had much less variance than for I_{Na}–Q_{on_max} measured from the same set of oocytes (Fig. 3 A).

The absolute magnitude of I_{Na}/Q_{on_max} observed in our oocyte studies was smaller than that anticipated from first principles of channel biophysics, even for WT channels. Starting with the assumptions that (a) the transition from fully closed to open is associated with the translocation of 12 elementary charges per channel (Hirschberg et al., 1995), (b) the peak open probability for $Na_V1.4$ is ∼0.2 (Cannon and Strittmatter, 1993), and (c) the unitary current is ∼1 pA, then the predicted ratio is:

$$\frac{I_{Na}}{Q_{on\_max}} = \frac{0.2 * (1pA/channel) * (10^{-6}\mu A/pA)}{(12e/channel) * (1.6 \times 10^{-10}\, nC/e)} = 104\ \mu A/nC.$$

Our observation for WT channels expressed in oocytes is about sixfold less, 17 µA/nC (Fig. 3). Comparative numbers are not widely available in the literature because for most studies optimized to measure Ig, the ionic current density is too high to maintain voltage-clamp control and therefore I_{Na} is not reported. In neuroblastoma cells, a whole-cell peak I_{Na} of −11 nA was recorded in 160 mM Na^+, after which block with TTX revealed a Q_{on_max} of 46 fC (Moran and Conti, 1990). These values are equivalent to a ratio of I_{Na}/Q_{on_max} = 240 µA/nC. In the squid giant axon, a Na^+ current density of 3.8 mA/cm^2 in 350 mM NaCl was associated with a charge displacement of 1,600 e/µm^2 for a voltage step from −70 to 20 mV (Bezanilla and Armstrong, 1976). The equivalent Q_{on_max}

is 25.6 nC/cm^2, and assuming that the Na^+ current density scales linearly with Na^+ concentration, it implies a ratio of I_{Na}/Q_{on_max} = 50 μA/nC in 120 mM Na^+. This latter value for an invertebrate preparation is within threefold of the value we measured for WT $Na_V1.4$ expressed in oocytes. The reason for the discrepancy is not immediately apparent; perhaps a mammalian Na^+ channel does not function efficiently in an amphibian expression system. Whatever the reason, this comparison to the behavior of endogenous channels illustrates the possible pitfall of estimating the I_{GP} density for HypoPP mutants expressed in mammalian fibers based on measurements in oocytes and assumptions about the ratio of I_{Na} to Q_{on_max}.

The measurement of I_{Na}, Q_{on_max}, and I_{GP} all from the same oocyte provides the information needed to predict the gating pore current density likely to occur in human HypoPP fibers, and also helps to resolve conflicting reports in the literature about the relative magnitude of I_{Na} and I_{GP} (Sokolov et al., 2007, 2010; Struyk and Cannon, 2007; Struyk et al., 2008). The preferred method for comparing the relative ease with which ions pass through the gating pore to that of Na^+ through the conventional central pore is by a ratio of unitary conductances, γ. This method avoids the influences of driving force and open probability. Assuming Ohmic behavior for both ion-conducting pathways and that the number of active channels in the membrane is proportional to Q_{on_max} (valid for I_{Na} of WT channels [Fig. 3 A, black circles] and for I_{GP} conducted by HypoPP mutants [Fig. 4 B]), we can write the ratio as:

$$\frac{\gamma_{GP\_mut}}{\gamma_{Na\_WT}} = \frac{I_{GP\_mut}/Q_{on\_max\_mut}}{I_{Na\_WT}/Q_{on\_max\_WT}} \times \frac{P_{o\_Na\_WT}}{P_{o\_GP\_mut}} \times \frac{V_{Na} - E_{Na}}{V_{GP} - E_{GP}},$$

where the subscripts on *V* indicate the voltage at which the Na^+ current or gating pore current were measured, V_{Na} = −25, and V_{GP} = −140 mV. The reversal potentials were E_{Na} = 45 mV and E_{GP} = 0 mV. We assumed $P_{o\_GP\_mut}$ = 1 at −140 mV, and used the published value of peak $P_{o\_Na\_WT}$ = 0.2 (Cannon and Strittmatter, 1993). The results of these calculations are summarized in Table 1. The relative conductance of the gating pore in HypoPP mutant channels to the conventional pore of a WT channel is ∼0.03% (see fourth row in Table 1). The unitary conductance of $Na_V1.4$ in 140 mM Na^+ is ∼20 pS (Cannon and Strittmatter, 1993), which implies that the unitary gating pore conductance is remarkably small, on the order of 10 fS.

Apparent discrepancies in the reported values for the relative amplitude of the gating pore and central Na^+ currents are primarily caused by different methods to describe the relative permeation of the two pathways. Sokolov et al. (2007) characterized the relative amplitude of the gating pore conductance for R672G as 1.2% for the central pore Na^+ current, based on currents recorded before and after the addition of TTX in one favorable oocyte where voltage-clamp control was sufficient. This value was calculated from a consideration of two physiological anchor points in skeletal muscle: the resting potential of −90 mV where for this oocyte, I_{GP} was 50 nA, and the peak of an action potential of 30 mV where in this case, I_{Na} was 4 μA. We initially estimated the ratio of the gating pore current to the peak Na^+ current for R669H to be ∼0.1% (Struyk and Cannon, 2007), based on the observation that the amplitude of I_{GP} (−140 mV) was ∼1/20th of the peak amplitude for the charge displacement current, Ig, which in turn is ∼50-fold smaller than the peak I_{Na} (Armstrong and Bezanilla, 1974). A similar conclusion of 0.1% was made for subsequent measures of I_{GP} for three other HypoPP mutations at R672H/S/C, now based on normalization to Q_{on_max} and the assumptions that each channel contributes 12 elementary charges and has a unitary current of 1 pA (Struyk et al., 2008). Subsequently, Sokolov et al. (2010) commented that including a peak P_{o_max} of 0.2 for $Na_V1.4$ in our calculation, and considering the possibility of partial I_{GP} block by divalent cations, may account for the 10-fold difference. With the extensive set of data in the present study where I_{Na}, Q_{on_max}, and I_{GP} were all measured in the same oocyte, there is now agreement that the relative amplitude of I_{GP} (−140) to the maximal peak I_{Na} for that same mutant channel is ∼1% (0.9–1.6%; Table 1, row 3). Our data also identify a defect in coupling between Q_{on_max} and I_{Na} for HypoPP mutant channels (Fig. 3), which would have caused the experimentally measured ratio to be about two to four times larger than predicted based on Q_{on_max} and coupling for WT channels. In our view, the more physiologically relevant measure is the conductance ratio of γ_{GP} in a HypoPP mutant to γ_{Na} in a WT channel. This unitary conductance ratio is ∼0.03% (Table 1, row 4). The 30-fold smaller value relative to the ratio of I_{GP}/I_{Na_mut} is accounted for by the multiplicative effects of peak P_o (fivefold), decoupling of charge displacement to channel opening (two- to fourfold), and the ratio of the driving forces at the two test potentials (twofold).

TABLE 1

Parameter estimates for the gating pore conductance

Parameter	Units	WT	R669H	R672G
I_{Na_max}/Q_{on_max}	nA/nC	17,400 ± 110	2,810 ± 360	6,460 ± 730
I_{GP}/Q_{on_max}	nA/nC	NA	25.6 ± 1.2	99.1 ± 5.5
I_{GP}/I_{Na_mut}	—	NA	0.0091	0.0155
$\gamma_{GP}/\gamma_{Na\_WT}$	—	NA	0.000174	0.000571
γ_{GP}: γ_{Na_WT}		NA	1:5, 750	1:1, 750
γ_{GP}[a]	fS	NA	2.95	11.4
Predicated GP conductance in HypoPP muscle				
G_{GP}[b]	μS/cm^2	NA	4.9	19.0
G_{GP}/G_{total}	—	NA	0.005	0.019

[a]Assumes γ_{Na_WT} = 20 pS.

[b]Assumes G_{Na_max} = 65 mS/cm^2 for WT $Na_V1.4$ in mammalian skeletal muscle.

Knowing the relative amplitudes for I_{Na}, Q_{on_max}, and I_{GP} in the same oocyte, we have greater confidence in estimating the magnitude of the anomalous gating pore conductance in human HypoPP muscle fibers. The predicted value is 5 μS/cm^2 for R669H and 20 μS/cm^2 for R672G. This calculation assumes that in heterozygous patients, WT and HypoPP $Na_V1.4$ alleles are expressed at the same level, as we have confirmed experimentally in a knock-in mouse model (Wu et al., 2011), and that the peak Na^+ conductance in mammalian skeletal muscle is 65 mS/cm^2 (Fu et al., 2011). This prediction of 5 μS/cm^2 for the R669H gating pore conductance in heterozygous patients is remarkably similar to the value of 7 μS/cm^2 we observed in homozygous R669H mutant mice (Wu et al., 2011). The measurement of I_{GP} in voltage-clamped mouse fibers was extremely challenging because of the difficulty in adequately blocking all of the normal ionic currents, and the concordance between the oocyte and fiber studies is an important confirmation. In HypoPP fibers, this gating pore conductance will be active at the resting potential and would account for ∼0.5–2% of the total resting conductance. Although this may appear to be a small disturbance to the stability of the resting potential, computer simulation has shown that the resulting inward current is sufficient to create a susceptibility to paradoxical depolarization in low-normal extracellular K^+ levels (Struyk and Cannon, 2008; Jurkat-Rott et al., 2010). The depolarized shift of the resting potential and inactivation of Na^+ channels cause loss of excitability and flaccid paralysis during transient attacks of weakness in HypoPP (Rüdel et al., 1984).

We thank Hillery Gray for technical assistance with oocyte preparation and David Francis for advice on recording gating pore currents.

This work was supported by grants from National Institute of Arthritis and Musculoskeletal and Skin Diseases of the National Institutes of Health (R37-AR42703) and the Muscular Dystrophy Association (MDA203224).

The authors declare no competing financial interests.

Kenton J. Swartz served as editor.

Submitted: 17 March 2014
Accepted: 19 June 2014

REFERENCES

Armstrong, C.M., and F. Bezanilla. 1974. Charge movement associated with the opening and closing of the activation gates of the Na channels. *J. Gen. Physiol.* 63:533–552. http://dx.doi.org/10.1085/jgp.63.5.533

Bezanilla, F., and C.M. Armstrong. 1976. Properties of the sodium channel gating current. *Cold Spring Harb. Symp. Quant. Biol.* 40: 297–304. http://dx.doi.org/10.1101/SQB.1976.040.01.030

Cannon, S.C. 2006. Pathomechanisms in channelopathies of skeletal muscle and brain. *Annu. Rev. Neurosci.* 29:387–415. http://dx.doi.org/10.1146/annurev.neuro.29.051605.112815

Cannon, S.C. 2010. Voltage-sensor mutations in channelopathies of skeletal muscle. *J. Physiol.* 588:1887–1895. http://dx.doi.org/10.1113/jphysiol.2010.186874

Cannon, S.C., and S.M. Strittmatter. 1993. Functional expression of sodium channel mutations identified in families with periodic paralysis. *Neuron.* 10:317–326. http://dx.doi.org/10.1016/0896-6273(93)90321-H

Capes, D.L., M. Arcisio-Miranda, B.W. Jarecki, R.J. French, and B. Chanda. 2012. Gating transitions in the selectivity filter region of a sodium channel are coupled to the domain IV voltage sensor. *Proc. Natl. Acad. Sci. USA.* 109:2648–2653. http://dx.doi.org/10.1073/pnas.1115575109

Francis, D.G., V. Rybalchenko, A. Struyk, and S.C. Cannon. 2011. Leaky sodium channels from voltage sensor mutations in periodic paralysis, but not paramyotonia. *Neurology.* 76:1635–1641. http://dx.doi.org/10.1212/WNL.0b013e318219fb57

Fu, Y., A. Struyk, V. Markin, and S. Cannon. 2011. Gating behaviour of sodium currents in adult mouse muscle recorded with an improved two-electrode voltage clamp. *J. Physiol.* 589:525–546. http://dx.doi.org/10.1113/jphysiol.2010.199430

Hirschberg, B., A. Rovner, M. Lieberman, and J. Patlak. 1995. Transfer of twelve charges is needed to open skeletal muscle Na^+ channels. *J. Gen. Physiol.* 106:1053–1068. http://dx.doi.org/10.1085/jgp.106.6.1053

Jurkat-Rott, K., N. Mitrovic, C. Hang, A. Kouzmekine, P. Iaizzo, J. Herzog, H. Lerche, S. Nicole, J. Vale-Santos, D. Chauveau, et al. 2000. Voltage-sensor sodium channel mutations cause hypokalemic periodic paralysis type 2 by enhanced inactivation and reduced current. *Proc. Natl. Acad. Sci. USA.* 97:9549–9554. http://dx.doi.org/10.1073/pnas.97.17.9549

Jurkat-Rott, K., B. Holzherr, M. Fauler, and F. Lehmann-Horn. 2010. Sodium channelopathies of skeletal muscle result from gain or loss of function. *Pflugers Arch.* 460:239–248. http://dx.doi.org/10.1007/s00424-010-0814-4

Lehmann-Horn, F., R. Rüdel, and K. Jurkat-Rott. 2004. Nondystrophic myotonias and periodic paralyses. *In* Myology. A.G. Engel and C. Franzini-Armstrong, editors. McGraw-Hill, New York. 1257–1300.

Matthews, E., R. Labrum, M.G. Sweeney, R. Sud, A. Haworth, P.F. Chinnery, G. Meola, S. Schorge, D.M. Kullmann, M.B. Davis, and M.G. Hanna. 2009. Voltage sensor charge loss accounts for most cases of hypokalemic periodic paralysis. *Neurology.* 72:1544–1547. http://dx.doi.org/10.1212/01.wnl.0000342387.65477.46

Moran, O., and F. Conti. 1990. Sodium ionic and gating currents in mammalian cells. *Eur. Biophys. J.* 18:25–32. http://dx.doi.org/10.1007/BF00185417

Rüdel, R., F. Lehmann-Horn, K. Ricker, and G. Küther. 1984. Hypokalemic periodic paralysis: In vitro investigation of muscle fiber membrane parameters. *MuscleNerve.* 7:110–120. http://dx.doi.org/10.1002/mus.880070205

Sokolov, S., T. Scheuer, and W.A. Catterall. 2007. Gating pore current in an inherited ion channelopathy. *Nature.* 446:76–78. http://dx.doi.org/10.1038/nature05598

Sokolov, S., T. Scheuer, and W.A. Catterall. 2010. Ion permeation and block of the gating pore in the voltage sensor of $Na_V1.4$ channels with hypokalemic periodic paralysis mutations. *J. Gen. Physiol.* 136:225–236. http://dx.doi.org/10.1085/jgp.201010414

Struyk, A.F., and S.C. Cannon. 2007. A Na^+ channel mutation linked to hypokalemic periodic paralysis exposes a proton-selective gating pore. *J. Gen. Physiol.* 130:11–20. http://dx.doi.org/10.1085/jgp.200709755

Struyk, A.F., and S.C. Cannon. 2008. Paradoxical depolarization of BA^{2+}-treated muscle exposed to low extracellular K+: Insights into resting potential abnormalities in hypokalemic paralysis. *Muscle Nerve.* 37:326–337. http://dx.doi.org/10.1002/mus.20928

Struyk, A.F., K.A. Scoggan, D.E. Bulman, and S.C. Cannon. 2000. The human skeletal muscle Na channel mutation R669H associated with hypokalemic periodic paralysis enhances slow inactivation. *J. Neurosci.* 20:8610–8617.

Struyk, A.F., V.S. Markin, D. Francis, and S.C. Cannon. 2008. Gating pore currents in DIIS4 mutations of NaV1.4 associated with periodic paralysis: Saturation of ion flux and implications for disease pathogenesis. *J. Gen. Physiol.* 132:447–464. http://dx.doi.org/10.1085/jgp.200809967

Townsend, C., and R. Horn. 1997. Effect of alkali metal cations on slow inactivation of cardiac Na^+ channels. *J. Gen. Physiol.* 110:23–33. http://dx.doi.org/10.1085/jgp.110.1.23

Townsend, C., H.A. Hartmann, and R. Horn. 1997. Anomalous effect of permeant ion concentration on peak open probability of cardiac Na^+ channels. *J. Gen. Physiol.* 110:11–21. http://dx.doi.org/10.1085/jgp.110.1.11

Wu, F., W. Mi, D.K. Burns, Y. Fu, H.F. Gray, A.F. Struyk, and S.C. Cannon. 2011. A sodium channel knockin mutant ($Na_V1.4$-R669H) mouse model of hypokalemic periodic paralysis. *J. Clin. Invest.* 121:4082–4094. http://dx.doi.org/10.1172/JCI57398

Wu, F., W. Mi, E.O. Hernández-Ochoa, D.K. Burns, Y. Fu, H.F. Gray, A.F. Struyk, M.F. Schneider, and S.C. Cannon. 2012. A calcium channel mutant mouse model of hypokalemic periodic paralysis. *J. Clin. Invest.* 122:4580–4591. http://dx.doi.org/10.1172/JCI66091